Trap-limited hydrogen diffusion in *a*-Si:H

Paulo V. Santos* and Warren B. Jackson
Xerox Corporation, Palo Alto Research Center, 3333 Coyote Hill Road, Palo Alto, California 94304
(Received 30 March 1992)

Hydrogen transport in *a*-Si:H was investigated by deuterium diffusion experiments where the deuterium source was either a remote atomic deuterium plasma or a deuterated amorphous silicon layer. An enhanced hydrogen diffusion and a considerably lower diffusion activation energy (0.5 eV instead of 1.2–1.5 eV) is observed for diffusion from a plasma. This behavior is attributed to saturation of hydrogen configurations with high binding energy, which act as deep hydrogen traps and control hydrogen transport in diffusion experiments from a deuterated layer, by deuterium atoms injected from the plasma. Diffusion from a plasma is then dominated by hopping through states with low binding energy. A density-of-states distribution is derived for the hydrogen configurations controlling diffusion consisting of (i) a shallow state where hydrogen is weakly bonded and can diffuse with a small activation energy of 0.5 eV and (ii) deep states with binding energy larger than 1.2 eV and a total density of $\sim 10^{22}$ cm^{-3}. In glow discharge *a*-Si:H, hydrogen is bonded to deep states and only a relatively small fraction (20–60 %) of these states are empty.

I. INTRODUCTION

Hydrogenated amorphous silicon (*a*-Si:H) has a high hydrogen concentration, and its structural and electronic properties are expected to depend on hydrogen transport. The *a*-Si:H structure has been described as a network of silicon atoms where hydrogen can move relatively easily at low temperatures.[1,2] Hydrogen diffusion plays a fundamental role during glow-discharge deposition of *a*-Si:H when a considerable amount of hydrogen is eliminated from the growing film.[3,4] In addition, since the low spin density found in electronic quality *a*-Si:H is due to hydrogen passivation of silicon dangling bonds, metastable changes in defect concentration are expected to be closely related to hydrogen motion.[5]

In this paper we investigate hydrogen transport in *a*-Si:H by analyzing deuterium and hydrogen diffusion profiles measured by secondary-ion-mass spectrometry (SIMS). In the diffusion experiments, the deuterium source was either a remote D_2 plasma (gas-phase source) or a deuterated *a*-Si:H layer (solid diffusion source). In agreement with previous investigations,[6–9] hydrogen diffusion properties were found to be significantly different in the two cases: diffusion from the plasma is a faster process, with an activation energy $E_a = 0.5$ eV much smaller than for diffusion from a deuterated layer ($E_a = 1.2-1.5$ eV). We attribute the differences to a strong dependence of the diffusion coefficient on hydrogen concentration. In the case of diffusion from a layer, the total concentration of hydrogen plus deuterium is kept approximately constant during diffusion, since both species diffuse in opposite directions with approximately the same diffusion coefficient. The hydrogen concentration profile is a complementary error function, indicating that the diffusion coefficient is concentration independent. For diffusion from the plasma, the total concentration of the two species increases during diffusion, as deuterium atoms are injected from the gas source. The extra deuterium atoms saturate silicon-hydrogen binding configurations with high binding energy, which control diffusion under constant concentration conditions. Diffusion then proceeds through other hydrogen configurations with low binding energies and smaller temperature activation. The diffusion profiles deviate significantly from the case of diffusion from a layer and exhibit a sharp cutoff, indicative of a concentration-dependent diffusion coefficient. The results are used to derive the energy distribution of silicon-hydrogen configurations controlling hydrogen transport in device quality *a*-Si:H.

This paper is organized as follows. Section II briefly describes sample preparation and the procedure followed in the diffusion measurements. Experimental results on the concentration profiles for hydrogen and deuterium after diffusion obtained by SIMS are presented in Secs. III A and III B. In Sec. III C we summarize results on hydrogen and deuterium bonding obtained by Raman spectroscopy. The experimental results are used in Sec. IV A to construct a model for hydrogen transport through the silicon network based on a distribution of silicon hydrogen binding energies. The hydrogen and deuterium profiles expected from the diffusion model are compared to the experimental results in Sec. IV B. Section IV C discusses the connection between hydrogen transport and the growth process, and Sec. V summarizes the main conclusions of this work.

II. EXPERIMENT

The *a*-Si:H samples used in the diffusion studies were grown by glow-discharge decomposition of pure silane on crystalline silicon substrates at 230 °C. Hydrogen transport in these samples was investigated by analyzing deuterium concentration profiles after deuterium diffusion at

different temperatures between 150 and 400 °C. Two sorts of deuterium sources were used. In the first case, single *a*-Si:H layers exposed to monatomic deuterium produced in an optically isolated, remote deuterium plasma at a constant pressure of 2.0 torr.[10] The deuterium plasma was generated in a microwave cavity upstream from the samples. Before (and also after) each deuteration, the samples were rinsed in diluted HF to remove any surface oxide that could form a barrier to deuterium incorporation.

Diffusion experiments were also performed using a solid deuterium source. In this case, the *a*-Si:H layers were capped *in situ* with a 200-nm-thick *a*-Si:H:D layer, obtained by diluting silane with a 20% volume fraction of deuterium, followed by a 100-nm-thick *a*-Si:H top layer. Both capping layers were deposited at 130 °C in order to reduce hydrogen diffusion during sample growth. The samples were then annealed either in vacuum or in air, for different temperatures and times.

The concentration profiles of deuterium and hydrogen after diffusion were determined by SIMS using Cs^+-ion bombardment and monitoring negative secondary ions. The conditions for the SIMS measurements were adjusted to yield a depth resolution of $x_r \sim 8$ nm for each factor of e of concentration decay at profiling depth of ~ 200 nm. The hydrogen and deuterium concentrations were calibrated using a standard crystalline silicon sample with a hydrogen implantation dose of 1×10^{14} cm^{-3}. The absolute concentration values reported here are accurate to within a factor of 2, but the relative precision of the SIMS measurements when comparing two different profiles is much better than that. The depth scales in the concentration profiles were obtained by measuring the depth of the craters formed during the ion bombardment with a stylus profilometer and are accurate to within 10%.

III. RESULTS

A. Diffusion from the plasma and a deuterated layer

Typical D concentration profiles of the multilayer structures used in diffusion experiments from *a*-Si:H:D layers are illustrated by the thin line in Fig. 1. The deuterium concentration decays from $\sim 5-7\times10^{19}$ cm^{-3} in the *a*-Si:H:D layer, corresponding to 1–2 at. % relative to the concentration of silicon atoms, to $\sim 5\times10^{17}$ cm^{-3} in the *a*-Si:H layer. The latter concentration corresponds to the natural D abundance in *a*-Si:H films with 10% hydrogen. Diffusion is negligible for temperatures below 200 °C, and the deuterium concentration profiles are indistinguishable from those in unannealed samples. The exponential concentration profile at the interface between the *a*-Si:H:D and *a*-Si:H layers is determined in this case by the depth resolution of the SIMS measurements. The resolution is limited by material intermixing during ion bombardment[11] to a minimal concentration decay length of 8.0 nm at a profiling depth of 200 nm. Above 200 °C [curves (c) and (d) in Fig. 1] diffusion becomes appreciable, and the concentration profiles at the interface between the two layers deviate from an exponential.

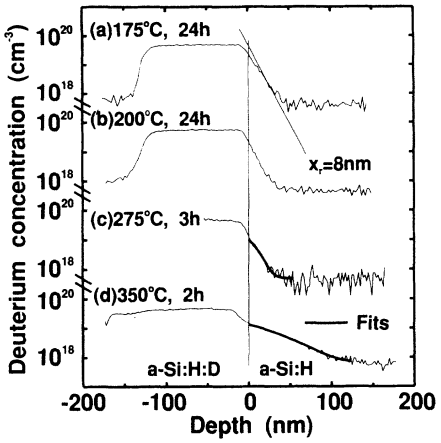

FIG. 1. SIMS concentration profile for deuterium in *a*-Si:H/*a*-Si:H:D/*a*-Si:H structures (thin solid lines) after diffusion at different temperatures. In (c) and (d) the heavy lines are complementary error function profiles fitted to the experimental data. The diffusion temperature and diffusion time are indicated for each curve and the vertical line marks the interface between the *a*-Si:H:D and *a*-Si:H layers.

The thin lines in Fig. 2 show corresponding profiles for diffusion from a deuterium plasma. Even for temperatures as low as 175 °C there is considerable deuterium incorporation from the plasma. In order to compare different diffusion profiles, we define an effective diffusion length x_0 as the depth where the deuterium concentration profile in the *a*-Si:H layer falls to 16% of the concentration at the boundary of that layer. At a given temperature, the diffusion length for diffusion from the plasma (Fig. 2) is considerably larger than for diffusion from a layer (Fig. 1). This is especially true for diffusion temperatures below 200 °C, where negligible diffusion from a layer is observed. (Note the different diffusion times in Figs. 1 and 2.)

For a constant surface concentration and a

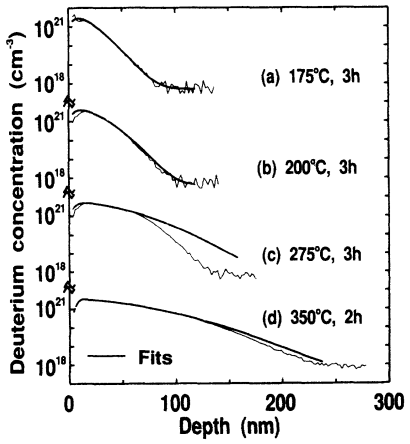

FIG. 2. SIMS concentration profile for deuterium diffused from a remote D_2 plasma in *a*-Si:H films at different temperatures. The thick lines are complementary error function profiles fitted to the experimental data.

concentration-independent effective diffusion coefficient D_{eff},the diffusion profile is a simple complementary error function (erfc), and the diffusion length is related to the diffusion time t_d by $x_0=2[(D_{\text{eff}}t_d)]^{1/2}$.[12] This is valid even if the diffusion coefficient is time dependent; in this case, D_{eff} is an average diffusion coefficient given by $D_{\text{eff}}=(1/t_d)\int D_{\text{eff}}(t')dt'$.[2] As will be discussed in detail later, this effective diffusion coefficient in a-Si:H takes into account both diffusion in mobile states and capture and release by hydrogen traps. The diffusion length for the low-temperature diffusion profiles in Figs. 1 and 2 is only a few times larger than the SIMS resolution x_r. By assuming the response function for the SIMS measurements $S(x)$ to be a simple exponential function with a characteristic decay distance $x_r=8.0$ nm, i.e.,[11]

$$S(x)=\exp(-x/x_r)/x_r\ , \tag{1}$$

the SIMS profiles are expected to follow a functional dependence given by

$$C(x)=C_s S(x)*\text{erfc}(x/x_0)\ , \tag{2}$$

where C_s is the concentration at $x=0$ and the asterisk stands for the convolution operation. Analytic expressions for $C(x)$ are given in the Appendix.

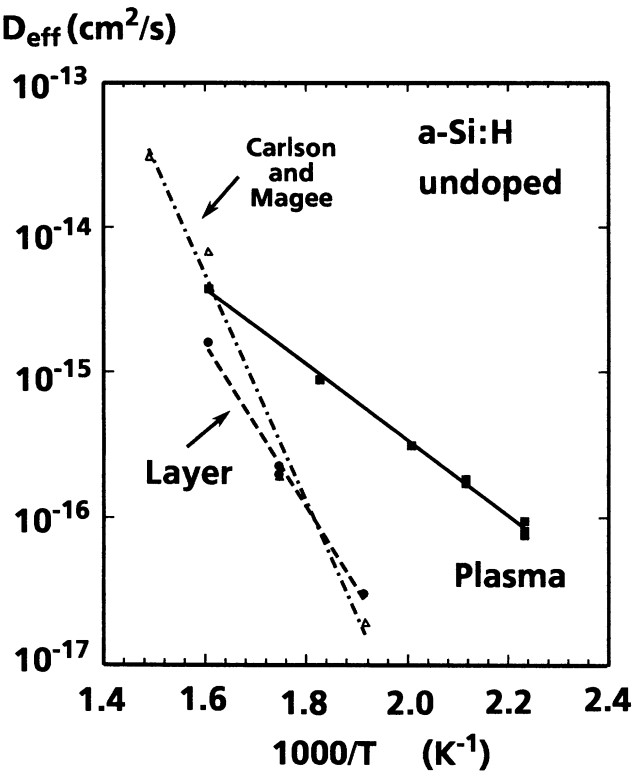

FIG. 3. Arrhenius plots for the deuterium diffusion coefficient from a solid source (circles, dashed line) and from a deuterium plasma (squares, solid line). The activation energies obtained from the slope of the lines are, respectively, 1.2±0.1 and 0.5±0.1 eV for the two diffusion processes. Also shown in the figure is the diffusion coefficient measured by Carlson and Magee for diffusion from a deuterated layer (triangles, dot-dashed line) with an activation energy of 1.53±0.15 eV (Ref. 14).

The thick lines in Figs. 1 and 2 were obtained by fitting the data to the function $C(x)$. The concentration profiles for diffusion from a layer are well reproduced by the function $C(x)$, indicating that the diffusion coefficient remains constant in this kind of diffusion. For diffusion from the plasma, a reasonable fit is only obtained for the high-concentration part of the profiles. For lower concentrations, the measured profiles decay faster than a complementary error function, in agreement with results reported previously by Sol and co-workers.[13] As will be discussed in detail later, this is due to the decrease in the diffusion coefficient with the total concentration of deuterium and hydrogen in the diffusion layer. The larger deviation from the fitting function occurs for temperatures below 300 °C: this deviation is not evident for temperatures below 200 °C in Figs. 2(a) and 2(b) because the concentration profiles in these cases are determined mainly by the SIMS resolution function [Eq. (1)], and deviations from a complementary error function profiles are not observable.

The diffusion coefficient determined from the fitting procedure for diffusion from a layer (circles) and from the gas phase (squares) are plotted in Fig. 3 as a function of inverse temperature. For comparison, the diffusion data obtained by Carlson and Magee for diffusion from an a-Si:H:D layer are also displayed (triangles).[14] For both types of deuterium sources, diffusion is thermally activated. For diffusion from a solid source, the diffusion coefficient has an activation energy of 1.2±0.1 eV and a prefactor between 10^{-6} and 10^{-5} cm^2/s. The activation energy is smaller than the 1.53-eV value reported by Carlson and Magee.[14] These authors reported a diffusion prefactor of 10^{-2} cm^2/s, which is three orders of magnitude larger than our measured value. Since in the low-temperature range ($T<350$ °C) their diffusion results essentially coincide with ours, we attribute these differences to the lower (and narrower) temperature range used by us for the determination of the activation energy and prefactor. Note that larger errors are involved in the calculation of the prefactor when diffusion data measured in a narrow temperature region are extrapolated to $1000/T\rightarrow 0$.

For low temperatures (below 300 °C), the diffusion coefficient for diffusion from the plasma is at least an order of magnitude larger than from a deuterated layer. The activation energy (0.5 eV) and diffusion prefactors (10^{-10} cm^2/s) are also significantly different than for diffusion from a layer.

B. Concentration-dependent diffusion coefficient

In the previous section we demonstrated that diffusion from a deuterium plasma is considerably faster than from a deuterated layer. In addition, the deuterium concentration profiles for diffusion from the plasma depend strongly on the concentration of activated deuterium species in the gas phase, as indicated in Fig. 4. Here, the upper curve illustrates a typical deuterium profile obtained after exposure of an a-Si:H film to a remote deuterium plasma at 275 °C for 3 h. The lower curve was obtained under

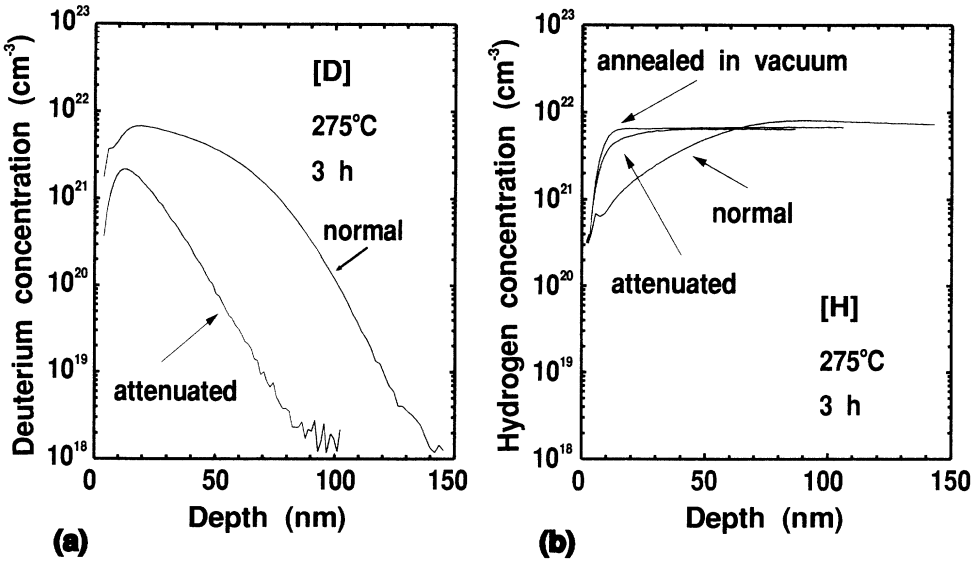

FIG. 4. (a) Deuterium concentration profiles in *a*-Si:H samples exposed to a normal (upper curve) and an attenuated (lower curve) deuterium plasma at 275 °C for 3 h. In (b) the corresponding hydrogen profiles for the same samples are shown, together with the hydrogen profile in a control sample annealed in vaccum under the same conditions.

the same annealing conditions, but for an attenuated concentration of activated deuterium atoms. The attenuation of monatomic species was achieved by (i) increasing the distance, and (ii) inserting a stainless-steel mesh in the path between the microwave plasma and the sample. Both procedures enhance the recombination of the activated species to form molecular D_2, thereby reducing the concentration of monatomic deuterium at the sample surface.[15,16]

As discussed previously, the concentration profiles for diffusion from the plasma deviate appreciably from a complementary error function. The deviations are even larger for an attenuated concentration of monatomic deuterium, as illustrated in Fig. 4(a). The profile in this case is a simple exponential function with a decay length determined by the SIMS depth resolution of ~8.0 nm. The plateau region near the surface, observed in the upper curve of Fig. 4(a), is completely absent for reduced deuterium concentration. A reduction in surface concentration does not lead to a simple renormalization of the depth scale of the diffusion profiles, as would be expected for a concentration-independent diffusion coefficient. When compared to diffusion from a deuterated layer, the effective diffusion coefficient for reduced deuterium concentration at 275 °C is enhanced by a factor of only 1.5–2, in comparison with a factor of ~10 enhancement for an unattenuated deuterium flux (see Fig. 3).

The diffusivity of the hydrogen initially present in the film is also affected by the monatomic deuterium concentration in the plasma. This behavior is illustrated in Fig. 4(b), where hydrogen concentration profiles for samples annealed at 275 °C in vacuum and exposed to normal and attenuated monatomic deuterium concentrations are compared. For the two last cases, the corresponding deuterium profiles are those of Fig. 4(a). Within the SIMS depth resolution, the hydrogen profile in the sample annealed in vacuum is indistinguishable from that of an unannealed sample [not shown in Fig. 4(b)], indicating negligible hydrogen out-diffusion. Except for the first 20–30 nm near the surface, the hydrogen profile does also not change appreciably in the sample exposed to an attenuated deuterium plasma. In the film exposed to a normal plasma, on the other hand, the hydrogen concentration decreases near the surface. The decrease is mainly due to hydrogen out-diffusion, but a fraction of the hydrogen atoms also diffuse towards the bulk, as will be discussed in more detail later. The enhanced deuterium diffusion from the plasma is therefore followed by a corresponding increase in hydrogen diffusivity. The characteristic diffusion length for hydrogen out-diffusion, defined here as the depth from the surface where the hydrogen concentration achieves 84% of the bulk values, is similar to the deuterium diffusion length, indicating that the two species have approximately the same diffusion coefficients in the deuterium-rich layer.

When single *a*-Si:H layers are exposed to a hydrogen plasma, the hydrogen concentration near the surface increases.[2] This behavior is illustrated in Fig. 5, where the hydrogen concentration in an *a*-Si:H layer exposed to a monatomic hydrogen plasma for 3 h at 275 °C is displayed. Near the sample surface, the hydrogen concentration in this case is almost 40% larger than in the bulk. Unfortunately, the hydrogen concentration in the first ~20 nm near the surface cannot be accessed due to the finite depth resolution of the SIMS measurements. Based on these results, one expects the total concentration of deuterium plus hydrogen to increase near the surface of a deuterated layer, if deuterium and hydrogen have similar diffusion properties in *a*-Si:H. This is indeed the case, as is illustrated in Fig. 6 for a sample exposed for 9 h to a deuterium plasma at 275 °C. Here, diffusion profiles for hydrogen [H] and deuterium [D] are shown,

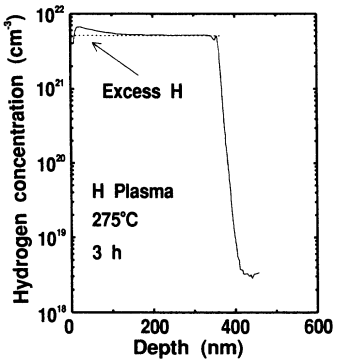

FIG. 5. Hydrogen concentration profile after exposure to a hydrogen plasma for 3 h at 275° C. This curve shows the increase in the hydrogen concentration near the surface due to hydrogen injection from the plasma.

together with the total concentration of deuterium plus hydrogen, [H+D]. Except in the first 20 nm near the surface, where the profiles are distorted by the finite SIMS resolution, the total concentration of deuterium plus hydrogen in the diffusion layer is up to ~100% larger than the original H concentration. The loss of hydrogen due to out-diffusion is overcompensated by the diffusion of deuterium from the plasma, leading to a net increase in the total concentration of the two species.

For comparison, Fig. 6(e) displays the deuterium profile for diffusion from a deuterated layer under the same conditions as for diffusion from the plasma. Note that in this case the diffusion coefficient is much smaller than for diffusion from the plasma.

A careful examination of Figs. 4(b) and 6(c) indicates that the hydrogen concentration after diffusion increases slightly beyond the bulk value in the region where the deuterium concentration drops. Such an accumulation is only possible if the hydrogen diffusion coefficient in the diffusion layer is significantly larger than in the bulk of the sample.[15] Under these conditions, hydrogen diffuses both towards the surface and towards the substrate, and accumulates at the border of the deuterium-rich layer, where the diffusion coefficient suddenly drops.

The increase in the total concentration of deuterium and hydrogen (D+H) near the surface, and the hydrogen pileup effect at the border of the diffusion layer, are not due to variations of the a-Si:H etch rate by the Cs^+-ion beam during SIMS profiling. Such a variation would be expected if the deuterium-rich layer had a higher etch rate then the rest of the material. To exclude this possibility, we monitor the ^{28}Si signal during a SIMS profile (see Fig. 6). The ^{28}Si concentration is depth independent, indicating a constant etch rate. In addition, transmission electron micrographs show that the a-Si:H layers are homogeneous, and no structural differences could be detected between the deuterium-rich layer had the underlining a-Si:H layer in deuterated samples.[17]

The region of enhanced diffusion coefficient is not confined to the immediate neighborhood of the surface, but propagates further into the material for increasing diffusion times, as is illustrated in Fig. 7. This figure shows deuterium profiles in a-Si:H films annealed at 275 °C for different times t_d in a remote deuterium plasma. For an annealing time of 9 h, the deuterium-rich layer extends more than 100 nm below the film surface. The deuterium profiles decay exponentially with depth for concentrations below $\sim 5\times10^{20}$ cm^{-3}, with a characteristic decay length of ~100 Å. The squares in the figure show the time dependence of the average diffusion coefficient obtained from the profiles. The diffusion coefficient decreases with increasing diffusion time. This behavior is well documented for hydrogen diffusion in a-Si:H and is attributed to the existence of a disorder-induced distribution of release times for diffusion.[18,19] For an exponential distribution of release times with characteristic width kT_0, the diffusion coefficient is ex-

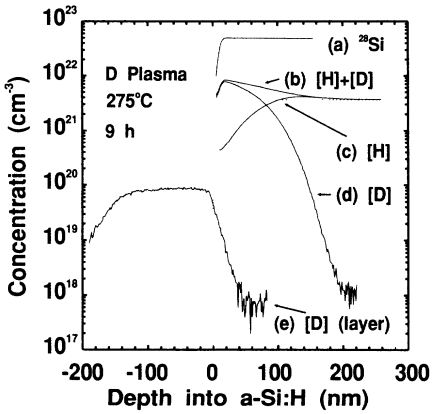

FIG. 6. SIMS concentration profiles for (a) ^{28}Si, (b) hydrogen, and (d) deuterium after exposure to a deuterium plasma for 9 h at 275 °C. Curve (c) displays the total concentration of deuterium plus hydrogen. For comparison, curve (e) shows the deuterium profile for diffusion from a deuterated layer under the same conditions.

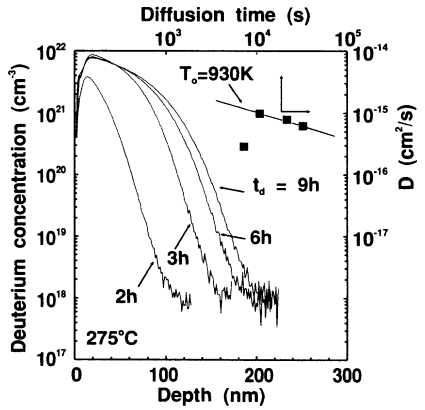

FIG. 7. Time dependence of the diffusion profiles for diffusion from a deuterium plasma (left and bottom axis). The diffusion experiments were performed at 275 °C and the diffusion times are indicated for each curve. The solid squares (right and upper axis) display the time dependence of the effective diffusion coefficient. The line through the squares corresponds to the expression $D_{\rm eff}\sim D_0(\omega t)^{1-T/T_0}$ with $T_0=930$ K (for details, see text).

pected to have a time dependence of the type[18]

$$D_{\text{eff}} \sim D_0(\omega t)^{1-T/T_0}, \tag{3}$$

where T is the absolute temperature, D_0 is a constant, and ω is a characteristic frequency. The solid line through the squares in Fig. 7 is a least-squares fit to the previous expression, which yields a characteristic temperature $T_0 \sim 930$ K. Characteristic temperatures T_0 between 600 and 1100 K have been reported for deuterium diffusion in a-Si:H, both from a deuterated layer or from a deuterium plasma.[15,20] This indicates that the decrease of the diffusion coefficient observed in Fig. 7 is not due to an increased distance from the surface, but rather to the dispersive nature of hydrogen diffusion in bulk a-Si:H.

C. Raman scattering

Structural information about hydrogen and deuterium bonding in deuterated a-Si:H samples was obtained by Raman spectroscopy. The Raman measurements were performed in the backscattering geometry using an excitation wavelength of 514.5 nm. For this wavelength, Raman spectroscopy probes a sample depth of ~ 50 nm, which is comparable to the diffusion length for the deuterium profiles in Fig. 1.

Figures 8(b)–8(e) display Stokes Raman spectra for a-Si:H samples exposed for 3 h to a deuterium plasma at different temperatures. For comparison, Fig. 8(a) shows the corresponding spectrum for an as-grown a-Si:H sample. The main lines in the spectra are associated with the excitation of (i) Si-Si transverse-optical-like (TO-like) vibration at $\omega_{\text{Si-Si}} = 480$ cm^{-1},[21] (ii) Si-H stretching vibration at $\omega_{\text{Si-H}} = 2010$ cm^{-1}, and (iii) S-D stretching vibration at $\omega_{\text{Si-D}} = 1470$ cm^{-1}.[22] The last mode is only present in deuterated samples and corresponds to the isotopic shift of the Si-H vibration when hydrogen is substituted for deuterium. Note that the frequency ratio $(\omega_{\text{Si-H}}/\omega_{\text{Si-D}} = 1.37)$ is close to the square root of the reduced mass ratio of the Si-D and Si-H bonds of 1.39.

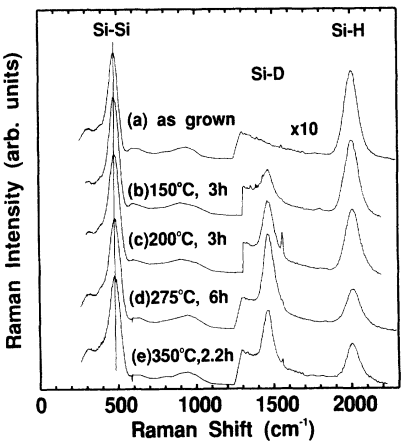

FIG. 8. (a)–(e) Raman spectra for a-Si:H samples exposed to a remote deuterium plasma for 3 h at different temperatures. The spectra were shifted vertically and Si-Si, Si-D, and Si-H denote the silicon-silicon TO-like vibration, the silicon-deuterium stretching mode, and the silicon-hydrogen stretching modes, respectively.

All spectra in Fig. 8 were normalized to the amplitude A_{480} of the TO-like vibration at 480 cm^{-1}. With increasing annealing temperature, the intensity of the Si-D vibration increases, while that of the Si-H mode decreases. This is in agreement with the SIMS result of the previous section, which demonstrate that deuterium incorporation is accompanied by hydrogen evolution from the film. The Si-H and the Si-D lines have a Gaussian shape with full width at half maximum (FWHM) of 147 ± 7 cm^{-1} and 115 ± 4 cm^{-1}, respectively. The ratio of the linewidths coincides with the frequency ratio between the two modes. No systematic change of the center frequency or the FWHM of the Si-D (or Si-H) with increasing deuterium content was observed. These results are in agreement with a previous study by Abeles and co-workers,[7,8] and indicate that the incorporated deuterium atoms occupy essentially the same sites as the hydrogen initially present in the film.

The integrated intensity of the Raman line for the localized Si-H, $I_{\text{Si-H}}$ vibration is related to the density $N_{\text{Si-H}}$ of scattering centers by the following expression:[23]

$$I_{\text{Si-H}} = \text{const}\,\omega_L(\omega_L - \omega_{\text{Si-H}})^3 A^2_{\text{Si-H}} N_{\text{Si-H}}, \tag{4}$$

where ω_L is the laser angular frequency and $A_{\text{Si:H}}$ is the vibration amplitude. A similar expression applies for the Si-D mode. Assuming the Si-H and Si-D bonds to have the same bond strength, the vibrational amplitudes of the two modes are inversely proportional to the square root of the reduced mass ratios, i.e., $A_{\text{Si-H}} \sim \sqrt{2} A_{\text{Si-D}}$. The normalized intensities, defined as $I^N_{\text{Si-H}} = \frac{1}{2}[(\omega_L - \omega_{\text{Si-D}})/(\omega_L - \omega_{\text{Si-H}})]^3 I_{\text{Si-H}}/A_{480}$ and $I^N_{\text{Si-D}} = I_{\text{Si-D}}/A_{480}$ are, therefore, proportional to the densities of Si-H and Si-D scattering centers, respectively. In Fig. 9 (lower curve) $I^N_{\text{Si-H}}$ is plotted as a function of $I^N_{\text{Si-D}}$ for a-Si:H samples deuterated at different temperatures. In agreement with the results of the previous sections, the Si-H concentration decreases with increasing Si-D density. The ratio of decrease of the Si-H density is smaller than that of decrease of the Si-H intensity. As a consequence, the total concentration of Si-H and Si-D scattering centers, proportional to $I^N_{\text{Si-H}} + I^N_{\text{Si-D}}$ and given by the upper curve in

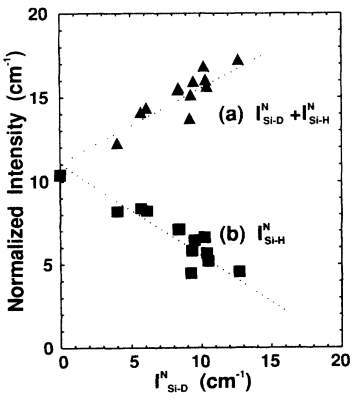

FIG. 9. Normalized integrated intensity of (a) hydrogen (I^N_{H}) and (b) hydrogen plus deuterium ($I^N_{\text{H}} + I^N_{\text{D}}$) determined from the intensity of the Raman lines as a function of the normalized deuterium integrated intensity (I^N_{D}).

Fig. 9, increases by ~30% for a factor-of-2 increase in the deuterium content ($I^N_{Si\text{-}D}$ increases from 5 to 10 cm^{-1}). If deuterium completely substitutes for hydrogen, the final deuterium concentration is expected from Fig. 9 to be twice as large as the original hydrogen concentration, in good agreement with the SIMS results of Fig. 6.

IV. DISCUSSION

The results presented in the previous section clearly demonstrate that deuterium has a higher diffusivity in a-Si:H when proceeding from a deuterium plasma than from a deuterated layer. The activation energy for the diffusion coefficient for diffusion from the plasma (0.5 eV) and the diffusion prefactor is substantially lower than for diffusion from a deuterated layer (see Fig. 3). Such small activation energies for diffusion from a gas source were reported by Nakamura *et al.* (0.3 eV),[9] and are also inferred from diffusion results presented by Widmer, Fehlmann, and Magee (0.35–0.75 eV).[6]

The increase in deuterium diffusivity is accompanied by a corresponding increase in the diffusivity of the hydrogen initially presented in the film. This leads to an enhanced hydrogen out-diffusion in a deuterium plasma. The in-diffusion of deuterium overcompensates for the hydrogen lost, and the total concentration of hydrogen plus deuterium in the diffusion layer is larger than the original hydrogen concentration. The diffusion coefficient in the deuterium-rich layer increases with the concentration of monatomic deuterium in the plasma, indicating a concentration-dependent process.

The increased hydrogen diffusion leads to hydrogen pileup at the interface between the deuterated layer and the original a-Si:H film (see Fig. 6). This can only occur if the enhancement in H diffusivity in the deuterium-rich layer is delayed relative to the deuterium incorporation; i.e., for short diffusion times, the hydrogen diffusion rate is smaller than that of deuterium. If the two rates were the same, no hydrogen accumulation would be seen, since a hydrogen concentration gradient would immediately build up near the surface, forcing deuterium to diffuse towards the surface.

The Raman results presented in Sec. III C indicate that the deuterium atoms incorporated from the plasma occupy essentially the same sites as the hydrogen initially in the film. No structural differences between the deuterium-rich and the underlining a-Si:H layer could be detected by TEM, indicating that the film structure remains essentially unchanged with deuterium incorporation.

Fast hydrogen diffusion from a plasma has been previously reported in the literature[6–9,24] and different explanations have been given for the diffusion-enhancement mechanism. Petrova and co-workers[24] attributed the fast hydrogen diffusion in glow-discharge a-Si:H films deposited at low temperatures (below 200 °C) to hydrogen motion on the internal surface of microvoids. High hydrogen diffusion was also observed in a-Si:H films with columnar structure and associated with a fast transport in the material between the columns.[24,25] Both diffusion mechanisms are based on material inhomogeneities and do not apply to the device-quality samples used in our study.

Rapid hydrogen diffusion from the plasma in this kind of material, together with a low diffusion activation energy, has been attributed to the fact that hydrogen (or deuterium) is moving through weakly bonded interstitial sites with low activation barrier for diffusion.[7–9] This requires that the capture of interstitial hydrogen by strongly bonded states is substantially reduced in the diffusion layer, leading to a longer lifetime in the interstitial states. In the next section we propose a model for hydrogen diffusion based in the existence of two sets of silicon-hydrogen configurations with different binding energies. According to the model, the enhanced lifetime in the shallow interstitials is due to the saturation of deep states by the extra deuterium atoms injected from the plasma. This leads to a strong dependence of the transport properties on the total concentration of deuterium plus hydrogen in the deuterated layer. In Sec. IV B we demonstrate, using computer simulations of the diffusion process, that the model basically reproduces all the experimental results presented in the last section.

A. Hydrogen configurations in a-Si:H

Hydrogen and deuterium diffusion from both solid- and gas-phase sources can be understood in terms of the distribution of silicon-hydrogen binding energies in the amorphous network depicted in Fig. 10.[15] Hydrogen diffuses by excitation over a barrier of height E_m, which represents the minimal energy for free hydrogen motion in the silicon network. Any disorder-induced broadening of the transport energy E_m is neglected here, and E_m is taken as the energy reference. As for the hydrogen glass model for a-Si:H,[1] we shall assume that the silicon network is a more or less rigid structure at the low diffusion temperatures used here, so that the possible hydrogen binding configurations do not change appreciably during hydrogen incorporation and diffusion. For simplicity, we also neglect any differences in binding energies for hydrogen and deuterium in a-Si:H.

Two sets of states are important for H transport: (i) shallow hydrogen states with low binding energy, where

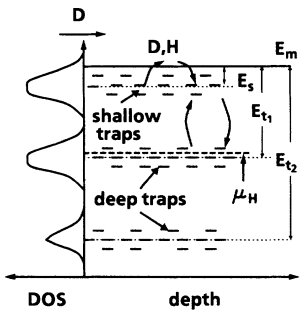

FIG. 10. Schematic representation of the density of states for hydrogen (left side) and of the spatial distribution of traps (right side) in the amorphous network. E_s and E_{ti} designate the different average trap energies, and E_m is the energy for mobile hydrogen. The population of the levels is assumed to be determined by a single hydrogen chemical potential μ_H.

hydrogen diffuses with a small diffusion activation energy E_s. As in crystalline silicon, these states are probably bond-center (BC) and interstitial (Td) sites in the silicon network. (ii) A collection of states with larger binding energies $E_{t1}, E_{t2}, \ldots < 1.2-1.5$ eV, corresponding to different silicon-hydrogen bonding configurations. Two of these configurations have been identified experimentally in hydrogen diffusion experiments: one ~ 1.2 eV below E_m, and a second one ~ 0.5 eV deeper.[15] Possible microscopic configurations for the different levels are discussed in detail in Refs. 15 and 26. The important point for the following discussion is that these hydrogen deep traps are energetically separated from the shallow ones by at least a few tenths of an eV.

An effective density of hydrogen states is depicted on the left side of Fig. 10. The distribution resembles that of electronic states in amorphous materials, and therefore one may expect hydrogen and electrons to have similar transport properties. In particular, the transport properties will depend on level occupation. This occupation can be described by an effective hydrogen chemical potential μ_H, which for simplicity will be assumed to be the same for the different hydrogen configurations. In as-grown a-Si:H films, μ_H lies just above the shallowest deep trap E_{t1} in Fig. 10. A relatively large fraction (60–80 %) of the deep traps are filled, and the total hydrogen concentration lies between 8 and 15 at. %. In diffusion experiments from a deuterated layer, the total concentration of H plus D remains fixed during diffusion, and the chemical potential is fixed at the deep trap level. Hydrogen transport is governed by hydrogen emission and recapture from deep traps, and the diffusion proceeds with an activation energy close to the energy separation between the transport level E_m and the shallowest occupied trap of $E_m - E_{t1}$, $\sim 1.2-1.5$ eV. Note that the activation energy normally differs from $E_m - \mu_H$ due to the temperature dependence of the chemical potential. The activation energy for diffusion can be significantly increased by removing hydrogen from the sample and bringing the chemical potential close to the deeper levels, as has been demonstrated in Ref. 15.

Diffusion from the gas phase differs from the previous case because the total concentration of hydrogen plus deuterium increases during diffusion, as shown in Figs. 5 and 6. The hydrogen chemical potential is then expected to move towards the shallow trap level (see Fig. 10). As proposed by Nakamura *et al.*,[9] diffusion can be substantially enhanced if the deep traps are saturated with extra deuterium atoms injected from the plasma. Under these circumstances, the deuterium atoms diffuse rapidly through the top deuterium-rich layer and are trapped at the interface with the bottom a-Si:H layer. Capture by traps at this interface leads to the fast-decaying, exponential-like profile at the border of the a-Si:H:D layer observed in Fig. 2.

Diffusion from the plasma in the presence of traps has been considered in detail by Herring and Johnson[27] for the case where hydrogen (and deuterium) reemission from deep traps can be neglected. This requirement is normally fulfilled at low diffusion temperatures; a more realistic situation, which takes into account trap reemission, will be discussed in the next section. For negligible trap reemission, the diffusion coefficient determined from the measured penetration depths, D_{eff} (see Fig. 3), differs from the actual diffusion coefficient in the deuterium-rich layer by a factor $\alpha^2 \sim C_{D,s}^{\text{surf}}/N_t^{\text{free}}$.[27] Here, $C_{D,s}^{\text{surf}}$ is the deuterium concentration in shallow traps near the surface, and N_t^{free} is the density of empty deep traps in the original a-Si:H film. The deuterium surface concentration in diffusion experiments from the plasma is weakly temperature dependent below 300 °C, indicating that α does not vary substantially with temperature.

The analysis presented above shows that the activation energy of 0.5 eV measured for diffusion from the plasma corresponds to that of a homogeneous layer with high hydrogen (or deuterium) content. This activation energy corresponds roughly to the energy difference $E_m - E_s$ between the transport and the shallow trap level in Fig. 10. The activation energy of 0.5 eV is also close to that for hydrogen diffusion in crystalline silicon, indicating that the average barrier height for diffusion is essentially the same in the two materials. This is a consequence of the similar short-range order in both materials.

With increasing hydrogen content, the hydrogen chemical potential in a-Si:H moves from a position close the deep trap level ($E_m - E_t \sim 1.2$ eV) to the proximity of the shallow traps level ($E_m - E_s \sim 0.5$ eV). Both Raman and SIMS results indicate that this shift requires an increase in the hydrogen-plus-deuterium density by a factor of 1.5–2. Since the original hydrogen concentration in the layers is $\sim 5\times 10^{21}$ cm^{-3}, the deep trap concentration N_t must be in the range $7-10\times 10^{21}$ cm^{-3} in the a-Si:H samples.

While the activation energy is not affected, the simple model discussed above indicates that the measured prefactor of the diffusion coefficient for diffusion from the plasma is reduced by a factor $\alpha^2 \sim C_{D,s}^{\text{surf}}/N_t^{\text{free}}$. In fact, the measured prefactor for diffusion from the plasma (10^{-10} cm^2/s) is substantially smaller than in crystalline silicon (10^{-2} cm^2/s) or for diffusion from a layer ($10^{-6}-10^{-5}$ cm^2/s). The lower prefactor for diffusion from the plasma arises from the fact that a substantial fraction of deuterium atoms injected from the surface is used to fill deep traps at the interface between the deuterated layer and the bulk a-Si:H film. The reduction factor α^2 can be estimated by recalling that when $C_{D,s}^{\text{surf}}$ equals the bulk equilibrium concentration of hydrogen in shallow traps given by $C_{H,s} \sim N_s \exp[-(E_{t1}-E_s)/kT]$, the in-diffusion of deuterium exactly compensates for the out-diffusion of hydrogen. Diffusion proceeds under constant concentration, and the diffusion coefficient is the same as for solid-source diffusion. According to Fig. 3, the two diffusion coefficients are equal at $T = 670$ K. Assuming N_s of the order of the density of interstitial (or bond center) sites is silicon ($N_s = 10^{23}$ cm^{-3}) and $N_t = 10^{22}$ cm^{-3}, we obtain $C_{D,s}^{\text{surf}}/N_t \sim 5\times 10^{-5}$ cm^2/s and $C_{D,s}^{\text{surf}} = 5\times 10^{17}$ cm^{-3}. This is roughly the ratio of 10^{-5} between the prefactors for gas- and solid-source diffusion.

The saturation of deep traps with increasing hydrogen concentration also accounts for the enhanced diffusion of the hydrogen initially present in the deuterated layer [see

Fig. 4(b)]. This occurs because once a hydrogen atom is released from a deep trap its lifetime in the shallow states is considerably longer. The enhancement in hydrogen diffusion lags that of deuterium because hydrogen initially occupies deep traps, while D is mostly in shallow states. The two diffusion coefficients become equal when the two populations thermalize. As discussed before, such a time lag is necessary to explain hydrogen accumulation at the interface between the deuterated and the bulk a-Si:H layer.

B. Numerical simulation of concentration profiles

In order to test the diffusion model presented in the last section, we simulated the diffusion profiles for hydrogen and deuterium by numerically solving the diffusion equation in the presence of traps. A simplified distribution of hydrogen configurations consisting of only two levels was used: a shallow transport level of energy E_s, and the shallowest of the deep traps level with energy E_t. The level densities are N_s and N_t, respectively. The diffusion process is described by the following set of equations:[15]

$$\frac{\partial C_{s,i}}{\partial t}=D_s\frac{\partial^2 C_{s,i}}{\partial x^2}-\frac{\partial C_{t,i}}{\partial t} \tag{5a}$$

and

$$\frac{\partial C_{t,i}}{\partial t}=\sigma[N_t-C_{\mathrm{H},t}-C_{\mathrm{D},t}]C_{s,i}-\nu N_s C_{t,i}\ , \qquad i=H,D \tag{5b}$$

where $C_{s,\mathrm{H}}$ ($C_{s,\mathrm{D}}$) and $C_{t,\mathrm{H}}$ ($C_{t,\mathrm{D}}$) are the hydrogen (deuterium) concentrations in shallow and deep traps, respectively. Equation 5(a) is the conventional Fickian diffusion equation with an additional term ($\partial C_{t,i}/\partial t$) to account for hydrogen (or deuterium) trapping in the deep states. The trapping rate is described in terms of a capture (σ) and emission (ν) probabilities for the deep traps. The capture probability is assumed to be related to the diffusion coefficient D_s in the shallow traps and to the capture radius r_c by $\sigma=4\pi D_s r_c$.[27] The capture and emission probabilities are related from detailed balance by the expression: $\nu=\sigma\exp[-(E_s-E_t)/kT]$.

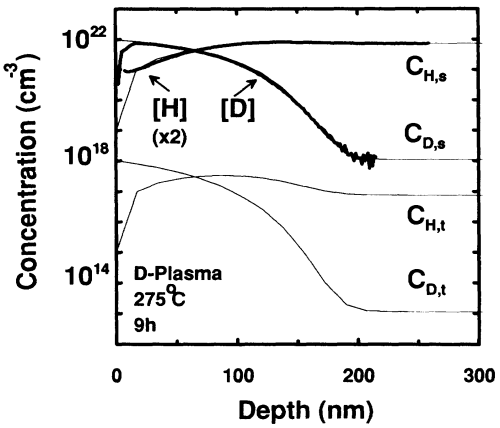

FIG. 11. Simulated hydrogen and deuterium concentration profiles (thin lines) in deep and shallow traps for a 9-h deuterium diffusion from the plasma at 275 °C. $C_{s,\mathrm{H}}$ ($C_{s,\mathrm{D}}$) and $C_{t,\mathrm{H}}$ ($C_{t,\mathrm{D}}$) are the hydrogen (deuterium) concentrations in shallow and deep traps, respectively. The thick lines reproduce the measured hydrogen (scaled by a factor of 2) and the deuterium profiles of Fig. 6.

Figure 11 shows the hydrogen and deuterium concentration profiles obtained by solving Eqs. 5(a) and 5(b) for the same diffusion time and temperature as the experimental data in Fig. 6 (reproduced by the thick lines in Fig. 11). The figure displays the hydrogen and deuterium concentrations in both shallow (index s) and deep (index t) traps. The diffusion coefficient was assumed to have an activation energy equal to the energy $E_s=0.5$ eV of the shallow traps and a prefactor of 0.3×10^{-6} cm^2/s. We assumed $N_t=10^{22}$ cm^{-3}, $N_s=10^{23}$ cm^{-3}, and an initial hydrogen concentration in the deep traps of $0.75N_t$. The boundary condition at the surface is determined by the hydrogen and deuterium concentration in shallow traps. These were taken to be 10^{15} and 10^{18} cm^{-3}, respectively. The latter value is close to the surface concentration of deuterium in shallow traps estimated in Sec. IV A. Finally, the capture radius for the deep traps r_c is not known: we assumed it to be equal to $\frac{1}{10}$ of the silicon-silicon bond length, i.e., $r_c=0.25$ Å.

The calculated profiles in Fig. 11 reproduce relatively well the main features. In the diffusion layer, all deep traps are occupied ([H]+[D]=N_t) and the deuterium profile is approximately given by a complementary error function. A sharp cutoff in the deuterium profile is seen at the edge of the diffusion region, where the diffusion coefficient decreases abruptly due to unsaturated traps. The abruptness of the diffusion profile at the border of the deuterated layer depends on the capture radius r_c and on the concentration of empty traps, $N_t^{\mathrm{free}}=N_t-C_{\mathrm{H},t}-C_{\mathrm{D},t}$.[15] If the product $N_t^e r_c$ is large, almost every deuterium atom reaching the border of the diffusion layer is captured by a deep trap, leading to a steep concentration profile. Diffusion does not proceed until the traps are saturated. As mentioned previously, the sharp drop in deuterium concentration is masked by the finite SIMS resolution in the experimental profiles.

The calculated hydrogen profile in Fig. 11 also exhibits a small hydrogen pileup at the edge of the diffusion layer. The calculations were performed for an initial hydrogen concentration a factor of 2 larger than the measured one. To account for that, the measure profile in Fig. 11 was also scaled by the same factor. The diffusion length for hydrogen out-diffusion is comparable to the deuterium penetration depth, indicating that the two species have similar diffusion coefficients, as noted before in connection with Fig. 6. The enhancement of diffusion for hydrogen initially presented in the film was attributed by Abeles and co-workers to a direct exchange mechanism, where deuterium in the mobile interstitial state is trapped by exchanging position with bonded hydrogen.[7,8] This process should cost little energy, since it does not require the break of a Si-H bond. For the energy distribution for the traps used in the simulations, such a direct exchange mechanism is not necessary to explain the enhanced hydrogen motion, since the thermal emission rate is already

sufficient to excite hydrogen to the shallow states.

The diffusion model described previously was also used to reproduce the differences in activation energy for solid- and gas-source diffusion. In this case, diffusion profiles for a fixed diffusion time t_d were calculated for the two kinds of diffusion by applying the appropriate set of boundary conditions to Eq. (1). The diffusion coefficient was then determined from the diffusion length x_0 using the relation $D_{\text{eff}}=x_0^2/4t_d$. The calculations were performed using the same set of parameters described previously. The results are summarized in Fig. 12 (lines), superimposed on the diffusion data from Fig. 3. For diffusion from a solid source (the dotted line in Fig. 12), an activation energy corresponding to the deep trap energy $E_t=1.2$ eV is obtained. The diffusion profiles in this case are well represented by a complementary error function and depend weakly on the capture radius r_c. The simulations of deuterium diffusion from the gas phase were performed for different values of the surface concentration deuterium in shallow traps, $C_{D,s}$, as shown by the solid lines in Fig. 12. For deuterium surface concentrations $C_{D,s}^{\text{surf}}>10^{17}$ cm^{-3} and temperatures below 350 °C, the effective diffusion coefficient for diffusion from the plasma is much larger than from a deuterated layer, reproducing the experimental results of Fig. 3. The diffusion activation energy is indicated near each line in Fig. 12 and increases with decreasing $C_{D,s}^{\text{surf}}$. For $C_{D,s}^{\text{surf}}>5\times10^{17}$ cm^{-3} the activation energy is substantially smaller than for diffusion from a layer and is comparable to the shallow trap energy of $E_s=0.5$ eV, in agreement with the results presented in Sec. III A. The changes in activation energy arise from the rapid statistical shift of the chemical potential with concentration from near the deep trap level to the shallow level for changes of a factor of 2 or less in the total concentration of deuterium plus hydrogen.

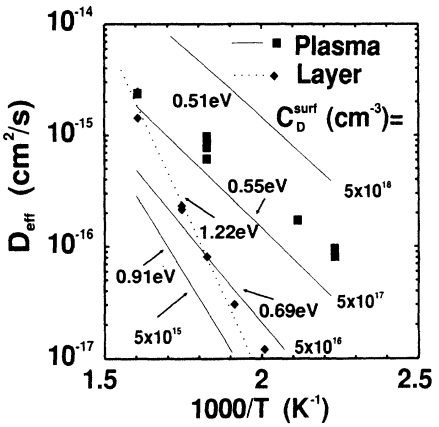

FIG. 12. Arrhenius plots for the effective diffusion coefficient D obtained from simulated diffusion profiles using the model described in the text, superimposed on the measured diffusion coefficient for diffusion from a deuterated layer (dots) and from a deuterion plasma (squares). The solid line represents the diffusion coefficient for diffusion from an a-Si:H:D layer. The dashed lines show the diffusion coefficient from the gas phase for different surface concentrations of deuterium in shallow traps, $C_{D,s}^{\text{surf}}$. The effective activation energies are displayed near each curve.

If at a given temperature the surface concentration $C_{D,s}^{\text{surf}}$ lies below the equilibrium concentration of hydrogen atoms in shallow traps, the out-diffusion of hydrogen may dominate over the in-diffusion of deuterium, depending on the details of the surface evolution boundary conditions. The occupancy of deep traps decreases below the level in the bulk, and the diffusion coefficient near the surface reduces below that for diffusion from a layer. This behavior is evident in Fig. 12 for surface concentrations $C_{D,s}^{\text{surf}}<5\times10^{16}$ cm^{-3}. Such conditions are met, for instance, when a-Si:H films are annealed in vacuum. The precise relationship between the diffusion coefficient and hydrogen concentration depend on the details of the energy distribution of deep traps: one expects, however, the hydrogen out-diffusion to be self-limiting, since the formation of a hydrogen-depleted layer near the surface restricts further hydrogen evolution. There is evidence for an energy barrier for the interchange of hydrogen and deuterium with the vacuum. Hydrogen evolution from the surface is believed to be limited by surface desorption of H_2 molecules. The concentration dependence of bulk diffusion described above may provide an additional barrier to hydrogen out-diffusion.

C. Hydrogen diffusion and the growth process

According to the model presented in the previous section, the strong dependence of the hydrogen diffusion coefficient on hydrogen concentration relys on (i) a large energetic separation between shallow and deep traps, and (ii) an original hydrogen concentration close to the deep trap density. The deep trap population determines the diffusion properties under constant concentration conditions, and, in particular, the diffusion activation energy. Small variations (i.e., of a factor of 1.4–2) in total hydrogen content, as in the case of diffusion from the plasma, and/or in trap concentration, should therefore induce larger changes in hydrogen transport properties. Diffusion measurements under constant concentration conditions (layer diffusion) on a-Si:H grown under different conditions, however, yield activation energies that lie invariably in a narrow range between 1.2 and 1.5 eV. This result indicates that the filling of the trap levels in as-grown samples should depend weakly on the deposition conditions.

This close relationship between trap density and hydrogen concentration is a probable consequence of the growth mechanism for a-Si:H. According to Robertson and Gallagher,[4] the growing surface of a glow-discharge film consists of a thin (some tens of Å), hydrogen-rich layer created by incorporation of radicals from the plasma. The silicon network formation occurs as hydrogen is eliminated through diffusion to the growing surface. The final structure of the a-Si:H depends on the balance between film growth rate and hydrogen elimination velocity.[3,28] Under the deposition conditions for electronic quality a-Si:H, most loosely bonded hydrogen atoms are expected to be eliminated from the silicon network. The remaining hydrogen is bonded in relative strong silicon hydrogen configurations, corresponding to the deep traps

in Fig. 10, and the hydrogen content in the final network is expected to be close to the trap density. It is therefore not surprising that the deep traps can be saturated by increasing the hydrogen concentration by only a few tens of percent.

Finally, the extra deuterium density necessary to saturate the deep traps in diffusion experiments from the plasma is on the order of $2-5\times10^{21}$ cm^{-3}. Raman measurements on the samples investigated here indicate that the extra deuterium atoms are bonded to silicon in the same way as hydrogen. The extra deuterium density is much larger than the dangling-bond density in a-Si:H, which is less than 10^{17} cm^{-3} even at the highest diffusion temperature reported here.[29] The extra hydrogen (or deuterium) atoms cannot, therefore, be trapped in existing silicon dangling bonds. The incorporation of the additional atoms probably takes place through the conversion of silicon-silicon bonds into two silicon-hydrogen bonds.[1] The previously proposed H_2^* pairing model is also consistent with such observations.[30] The lack of significant decrease in the silicon TO peak (see Fig. 8) suggests that normal Si-Si bonds are broken in order to accomodate the hydrogen in Si-H bonds. The incorporation process does not create extra silicon dangling bonds and leads to a pinning of the hydrogen chemical potential, since new hydrogen configurations can always be created at the expense of weak silicon-silicon bonds. Under these circumstances, the diffusion coefficient should remain concentration independent. The saturation levels found here for the maximum density of deep traps impose an upper limit of $\sim5\times10^{21}$ cm^{-3} to the maximum density of silicon bonds that can be converted to silicon-hydrogen bonds.

V. CONCLUSIONS

We have investigated hydrogen transport in undoped a-Si:H films by performing deuterium diffusion experiments from either a gas-phase source (deuterium plasma) or from an a-Si:H:D layer. Information about hydrogen diffusion was then obtained by analyzing SIMS diffusion profiles for both hydrogen and deuterium. The main conclusions of this work are summarized as follows:

(a) The diffusion coefficient for diffusion from a deuterium plasma is substantially larger than for diffusion from a deuterated layer. In the temperature range from 200 to 350 °C, the activation energies for the two processes are 0.5 and 1.2±0.1 eV, respectively.

(b) The larger diffusion coefficient for diffusion from the gas phase is attributed to the saturation of deep hydrogen (deuterium) traps by the extra deuterium atoms injected from the plasma. After trap saturation, diffusion proceeds through silicon-hydrogen configurations with low binding energies. These two sets of configurations are energetically separated by at least 0.5 eV.

(c) The hydrogen diffusion process is well explained by a hydrogen density of states consisting of two main levels: (i) a shallow (i.e., with low binding energy) state, with a binding energy of 0.5 eV. These hydrogen configurations are probably hydrogen interstitials and at silicon-silicon bond centers, and (ii) deep hydrogen traps, with binding energies above 1.2 eV. Different sets of deep levels may exist, corresponding to different hydrogen-silicon binding configurations.

(d) The total concentration of deep centers depends on the growth conditions and is larger (20–60 %) than the hydrogen content in the film.

ACKNOWLEDGMENTS

We thank R. A. Street and E. Tarnow for helpful discussions and for comments on the manuscript. We are grateful to R. Thompson and C. C. Tsai for sample preparation, and to G. Anderson for the TEM micrographs. The research was supported by the NREL (Golden, CO).

APPENDIX

As stated in Eq. (2), the measured SIMS profiles $C(x)$ represent the convolution of a complementary error function and the resolution function for the SIMS analysis, given by Eq. (2). The convolution operation can be evaluated analytically, leading to the following expression for the function $C(x)$:

$$C(x)=C_s\left[\operatorname{erfc}\left[\frac{x}{x_0}\right]+F\right]. \tag{A1}$$

The factor F depends on boundary conditions at the beginning of the diffusion layer. For diffusion from a deuterated layer, F is given by

$$F=\exp\left[\frac{x_0^2}{4x_r^2}-\frac{x}{x_r}\right]\operatorname{erfc}\left[\frac{x_0}{2x_r}-\frac{x}{x_0}\right], \tag{A2}$$

where the origin of the x axis is assumed to be the interface between the deuterated and hydrogenated layers. For diffusion from the plasma, the following expression holds:

$$F=\exp\left[-\frac{x}{x_r}\right]\left\{\exp\left[\frac{x_0^2}{4x_r^2}\right]\left[\operatorname{erfc}\left[\frac{x_0}{2x_r}-\frac{x}{x_0}\right]-\operatorname{erfc}\left[\frac{x_0}{2x_r}\right]\right]-1\right\}. \tag{A3}$$

*On leave from the Physics Institute, Universidade Estadual de Campinas, Campinas, São Paulo, Brazil.

[1] R. A. Street, in *Amorphous Silicon Semiconductors—Pure and Hydrogenated,* edited by A. Madam, M. Thompson, D. Adler, and Y. Hamakawa, MRS Symposia Proceedings No. 95 (Materials Research Society, Pittsburgh, 1987), p. 13.

[2] J. Kakalios and W. B. Jackson, in *Amorphous Silicon and Related Materials,* edited by Hellmut Fritzsche (World

Scientific, Singapore, 1988), p. 207.
[3]R. A. Street, Phys. Rev. B **43**, 2454 (1991).
[4]R. Robertson and A. Gallagher, J. Appl. Phys. **59**, 3402 (1986).
[5]W. B. Jackson and J. Kakalios, Phys. Rev. B **37**, 1020 (1988).
[6]A. E. Widmer, R. Fehlmann, and C. W. Magee, J. Non-Cryst. Solids **54**, 199 (1983).
[7]B. Abeles, L. Yang, D. Leta, and C. Majkrzak, J. Non-Cryst. Solids **97&98**, 353 (1987).
[8]B. Abeles, L. Yang, D. P. Leta, and C. Majkrzak, in *Interfaces, Superlattices and Thin Films,* edited by J. D. Dow and I. Schuller, MRS Symposia Proceedings No. 77 (Materials Research Society, Pittsburgh, 1987), p. 623.
[9]M. Nakamura, T. Ohno, K. Miyata, N. Konishi, and T. Suzuki, J. Appl. Phys. **65**, 3061 (1989).
[10]N. M. Johnson, in *Hydrogen in Semiconductors, Semiconductors and Semimetals,* edited by J. L. Pankove and N. M. Johnson (Academic, San Diego, 1991), Vol. 34, p. 113.
[11]R. G. Wilson, F. A. Stevie, and G. W. Magee, *Secondary Ion Mass Spectroscopy—A Practical Handbook for Depth Profiling and Bulk Impurity Analysis* (Wiley, New York, 1989).
[12]B. Tuck, *Introduction to Diffusion in Semiconductors* (Peregrinus, Salisbury, 1974).
[13]N. Sol, D. Kaplan, C. Dieumegard, and D. Dubreuil, J. Non-Cryst. Solids **35&36**, 291 (1980).
[14]D. E. Carlson and C. W. Magee, Appl. Phys. Lett. **33**, 81 (1978).
[15]W B. Jackson and C. C. Tsai, Phys. Rev. B **45**, 6564 (1992).
[16]N. M. Johnson, P. V. Santos, J. Walker, and K. S. Stevens, in *Amorphous Silicon Technology—1991,* edited by A. Madam, Y. Hamakawa, M. J. Thompson, P. C. Taylor, and P. G. LeComber, MRS Symposia Proceedings No. 219 (Materials Research Society, Pittsburgh, 1991), p. 703.
[17]G. Anderson, private communication.
[18]J. Kakalios, R. A. Street, and W. B. Jackson, Phys. Rev. Lett. **59**, 1037 (1987).
[19]J. Shinar, R. Shinar, S. Mitra, and J.-Y. Kim, Phys. Rev. Lett. **62**, 2001 (1989).
[20]R. Shinar, X.-L. Wu, S. Mitra, and J. Shinar, in *Amorphous Silicon Technology—1991* (Ref. 16), p. 75.
[21]J. E. Smith, M. H. Bodsky, B. L. Crowder, M. I. Natham, and A. Pinczuk, Phys. Rev. Lett. **26**, 642 (1971).
[22]M. H. Brodsky, M. Cardona, and J. Cuomo, Phys. Rev. B **16**, 3556 (1977).
[23]J. S. Lanning, in *Semiconductors and Semimetals, Part B,* edited by J. I. Pankove, R. K. Willardson, and A. C. Beer (Academic, Orlando, 1984), Vol. 11, p. 159.
[24]V. Petrova-Koch, H. P. Zein, H. Herion, and W. Beyer, J. Non-Cryst. Solids **97&98**, 807 (1987).
[25]R. A. Street and C. C. Tsai, Philos. Mag. **57**, 663 (1988).
[26]W. B. Jackson and S. B. Zhang, in *Transport, Correlation, and Structural Defects,* edited by H. Fritzsche (World Scientific, Singapore, 1990), p. 63.
[27]C. Herring and N. M. Johnson, in *Hydrogen in Semiconductors, Semiconductors and Semimetals* (Ref. 10), p. 225.
[28]K. Winer, Appl. Phys. Lett. **55**, 1759 (1989).
[29]R. A. Street and K. Winer, Phys. Rev. B **40**, 6236 (1989).
[30]S. B. Zhang, W. B. Jackson, and D. J. Chadi, Phys. Rev. Lett. **65**, 2575 (1990).